PREDICTING RICE FIELDS USING DEEP TABULAR LEARNING ALGORITHM

by

Subas Thapa
Student Number: 2128468

A dissertation submitted in partial fulfillment
of the requirements for the degree of
M.Sc. Data Science
(School of Engineering, Computing & Mathematical Sciences)
University of Wolverhampton
12 May 2023

TABLE OF CONTENTS

LIST OF FIGURES

Figure

LIST OF TABLES

Table

ABSTRACT

With the increasing availability of global satellite data, computing power and machine learning algorithms have paved the way to understand our planet better. In recent years, Machine Learning(ML) and Artificial Intelligence(AI) are the key factors in sustainable development. Satellite images have been used extensively in recent years to identify, classify, predict and monitor crop fields. Rice fields in An Giang province are mostly covered by clouds, making it difficult to obtain data from optical sensors. While Sentinel-1 Synthetic Aperture Radar(SAR) active sensors can monitor the earth's surface regardless of weather and environmental conditions at any time of day or night. This study explored the use of Sentinel-1 radar time-series data to monitor and identify whether the field is a rice field or not based on the Radar Vegetation Index(RVI) and backscattering coefficients. The experiment was carried out in 600 different locations in An Giang province. Sentinel-1 uses a C-band to capture images every 12 days. We obtained Sentinel-1 Radiometrically Terrain Corrected(RTC) data from Planetary Computer Hub starting from December 2021 till November 2022. RTC data in Planetary Computer are stored as cloud optimize GeoTIFF files. A bounding box of area 50X50 square meters was created for each location. Then, mean VV, VH, VRAT(VV/VH), SPAN(VV+VH), diff(VV-VH) and RVI4S1 values for a particular location are then calculated. SPAN calculates the total power received at both channels and can be calculated by adding VV and VH polarisations. The month value was also extracted for time series analysis. Data obtained from above is then fed into the TabNet model to classify the field. Our developed model is a binary classification supervised learning algorithm. Accuracy, precision, recall, and F1-Score received after applying

the TabNet algorithm are 84.5%, 81.2%, 86.8%, and 83.9% respectively. The variance of polarization and RVI values of rice fields are higher compared to non-rice fields. The proposed approach successfully predicted rice and non-rice fields with good accuracy scores using polarisation values and RVI. The dispersion of backscatter intensity of rice fields was found to be low compared to non-rice fields. Different phenological phases of rice such as vegetative, reproductive and ripening stages were detected. Additionally, the backscatter intensity of the river was found to be lowest due to specular reflection while residential areas have the highest due to double bounce scattering.

ACKNOWLEDGEMENTS

I would like to express my sincere gratitude to Professor Mr Adeel Ahsan for his guidance and feedback. I would also like to thank EY Open Science Data Challenge for conducting such a competitive challenge that helps to build a sustainable future. I would also like to thank Microsoft for providing access to the Planetary computer and Data catalogue. I am grateful and proud to have supportive parents and wife. Without them, it wouldn't have been possible. I like to take the opportunity to thank the Pytorch team who developed the TabNet package. Special thanks go to Dr. Resham Thapa, my Uncle who encouraged me to research this area.

CHAPTER 1

Introduction

In recent years, Machine Learning(ML) and Artificial Intelligence(AI) are the key contributors to sustainable development. The global economy and food security are under threat due to price volatility in the global agricultural market [17]. Due to industrialization and climate change, rice production is being undermined. As a result, farmers are changing agricultural practices such as the use of hybrid crops, fertilizers and water management. In order to fulfil the growing demand for food, farmers are turning practices to intensive farming with shorter crop cycles and higher production. Satellite data can be used to monitor the condition of crops and soil based on seasonal changes, and it can also help to predict harvests. Information about phenological development is the key to identifying and monitoring crop development stages. Additionally, it can identify excessive cultivation, soil degradation, improper irrigation and crop health so that provide food security can be provided to vulnerable areas. Most of the satellite data are easily accessible to the public. However, it requires huge memory and computation power to analyze the time series data. This research aims to identify the rice fields using Sentinel-1 Synthetic Aperture Radar(SAR) time-series data. Radar wavelengths can penetrate vegetation while optical wavelengths can't. This chapter will provide a brief introduction to our research topic, and background, followed by the research problem, objectives, aims and research questions, analysis, importance and limitations.

Sentinel-1 data was used to map nationwide rice fields in Thailand using the U-net model [39]. The U-net model is used for semantic image segmentation and classifying pixels [13]. Sentinel-1 SAR time series data were also used to identify rice fields in France using the decision tree and Random Forest(RF) algorithms based on polarization σ°_{VV} and σ°_{VH} [9]. Both Sentinel-1 SAR and Sentinel-2 optical data were used to extract rice fields in Mazandaran province in Iran [14]. Random Forest, XGBoost, 2 Dimensional- Convolutional Neural Networks(2D-CNN) and 3 Dimensional - Convolutional Neural Networks(3D-CNN) were used to identify rice fields and they proposed a

multi-stream framework [14]. Backscattering data σ°_{VV} and σ°_{VH} from Sentinel-1 were used to extract the wetland vegetation information [23]. Creating ground truth data for the U-net module is tedious and requires expertise. Additionally, identifying rice fields nationwide using deep learning requires huge memory and computing power. This paper will identify the rice fields using Sentinel-1 time-series data by applying a deep tabular learning algorithm, TabNet. Backscattering coefficients of rice and non-rice fields will also be analysed to detect various phenological phases of rice. Sentinel-1 Radiometrically Terrain Corrected(RTC) data, derived from Ground Range Detected(GRD), obtained from Microsoft Planetary Computer will be used in this research [26]. TabNet is a deep tabular learning algorithm and it outperformed XGBoost, Decision Tree, Random Forest and several other algorithms [5]. While most of the studies were conducted nationwide and require huge memory and computing power, this study focuses on small paddy fields. The dataset provided by EY Data Challenge consists of 600 locations in An Giang Province, classified as rice and non-rice fields. Polarization data(VV, VH) were obtained and mean RVI is calculated for a period(December 2021 to November 2022).

Most of the research in past is based on Decision Tree, Random Forest, and K-Means clustering algorithms to classify the location. However, this study aims to identify and classify whether the field is a rice field or a non-rice field based on the TabNet algorithm. The main objective of this research is to understand the relationship between backscattering coefficient values with rice phenology, growth and structure. This research also aims to explore more about how the radar backscatter intensities provide information about the rice crop cycle and stage information. Additionally, time-series analysis of all features γ°_{VV}, γ°_{VH}, SPAN(γ°_{VV} + γ°_{VH}), diff(γ°_{VV} - γ°_{VH}), VRAT(γ°_{VV} /γ°_{VH}) and RVI4S1 will be explored [24].

This study will significantly impact understanding, identifying, monitoring and evaluating crop yields to better plan for food famine. It also adds insights into how droughts, floods and other extreme events affect the rice phenological cycle. By identifying such events we can manage food supply management in a better way. It helps to lay a foundation to deploy smart crop management practices and helps to optimize inputs like water, fertilizer and other important resources in crop management. By analyzing the vegetation index of rice plants, we can easily identify the health of the crop so that we can take corrective and preventive actions early. Climate change greatly influences agricultural practices and biodiversity. This research aims to help farmers or policymakers adapt, mitigate and implement new policies.

Our study only focuses on Sentinel-1 radar data of An Giang province, Vietnam at the moment. Sentinel-1 offers a dual-polarization mode and high temporal resolution.

Sentinel-2 optical data are not taken into consideration in our research. Clouds in optical data need to remove from the images and our ability to identify clouds in images is not perfect. As a consequence, data generated from the images having persistent clouds will impact the result of models.

CHAPTER 2

Study Area and Field Information

The study was carried out in 600 different locations in An Giang province, Vietnam. The dataset provided by EY Open Data Challenge 2023 consists of 300 locations of rice fields and 300 non-rice fields. This section will first present the area of our study and then the data used to carry out the research. Sentinel-1 Radiometrically Terrain Corrected(RTC) data provided by Microsoft will be used for our research. The backscatter values obtained from Sentinel-1 RTC datasets are gamma-nought. Sigma-nought values are normalised with respect to the incidence angle to obtain gamma-nought values.

2.1 Study Area and Ground Truth Data

Test site, An Giang Province located in the Mekong River delta in Vietnam. Rice is cultivated in 85% of agricultural fields in An Giang province [20]. Our study area locates from 10°120' to 10°570' N latitude and 104°460' to 105°350' E longitude [20]. Mekong River flows through An Giang province leading to abundant water resources.

Data provided by EY Data challenge consists of 600 different locations where 300 fields are classified as rice fields and another 300 fields as non-rice fields. Our locations are in three districts: Chau Phu, Chau Thanh and Thoai Son. Most of the areas are plain and are lying 0.7–1.2 m in height from the sea level [20].

2.2 Rice Crop Calendar

Most of the rice fields in An Giang province, Vietnam are cultivated three times a year as seen in Table 2.1. Harvesting of the rice crops is normally done in April, August and December. Some fields can have a shorter cycle while some may take longer to harvest depending on the rice species.

Rice Season	Sowing/Transplanting	Harvest
Winter-Spring	November-December	March-April
Summer-Autumn	April-May	July-August
Autumn-Winter	July-September	October-December

Table 2.1: Crop Life Cycle in An Giang Province, Vietnam Source: *Hoa et. al.*

CHAPTER 3

Literature Review

3.1 Introduction and Background

Active and passive are the two types of remote sensing observation. Passive measures the amount of energy emitted or reflected by the Earth's surface while active sensors illuminate signals and record the portion of signals as a backscatter. Active sensors also record the time required to reach back to the sensor as delay time. Optical(passive) remote sensors sense surface and canopy conditions, while radar(active) microwaves can penetrate the canopy [30]. Backscatter depends on the roughness and electrical conductivity of the surface. Longer wavelength radar signals such as L-band can penetrate highly dense forest canopies while C-band is perfect for paddy fields with low biomass vegetation [29].

Copernicus is an Earth observation program under European Union's Space programme. Sentinel data acquired by Sentinel satellites are provided for free. The European Commission(EC) and the European Space Agency(ESA) jointly launched satellites Sentinel-1A and Sentinel-1B in 2014 and 2016 respectively to monitor Earth and provide information about the land, ocean and ice zones [31]. SAR data have high revisit frequency and spatial resolution. Sentinel-1 satellites operate in SAR mode and use C-band(5.6cm) [29]. Ground Range Detected(GRD) and Single Look Complex(SLC) are two product types available by Copernicus Open Access Hub [12].

The radar consists of a transmitter, receiver and antenna and also has an electronic system to process and record the data generated by a transmitter [27]. Radar can measure strength and position as amplitude and phase respectively. The backscattering coefficient(sigma nought) also known as strength is measured in decibels(dB). Radar parameters frequency, polarisation and incidence angle influence the reflection [27]. The incidence angle is the angle between the direction of radar signals and the Earth's surface. Radar signals with large incidence angles will be more sensitive to the roughness of the Earth's surface and penetrate less as opposed to small incidence angles. Radar signals with smaller

incidence angles will penetrate more and result in high backscatter intensity [27]. Radar signals are sensitive to the dielectric properties of the surface and structure of the vegetation. According to the rule of thumb, the higher the backscatter intensity the rougher the surface. The amount of water in soil and vegetation can influence the radar reflectivity which is a result of low penetration of signals.

Data products can be categorised into three groups: Level-0, Level-1 and Level-2. Level-0 data are raw data that are unprocessed and compressed. Level-1 data are either Single-Look Complex(SLC) or Ground range detected Geo-Referenced(GRD). While level-2 data products are specially derived for the analysis of the ocean. Sentinel-1 operates and obtains data in four acquisition modes: Stripmap(SM), Interferometric Wide swath(IW), Extra-Wide swath(EW) and Wave(WV) [27]. Out of four modes, IW is the most widely used for land monitoring(forestry, agriculture) applications.

Backscatter intensities depend on incidence angle and position(near, or far). so the radar images need to be corrected for speckle and topographical effects. Based on incidence angle and position, some location appears brighter while some appear dark in SAR images. Firstly, due to the side-looking nature of SAR images, level-1 data products contain geometric distortion. Secondly, SAR images contain unwanted noise also known as speckle. Speckle noise is a grainy salt-and-pepper pattern present in SAR images. Preprocessing of data is necessary to remove noise from the images.

3.2 SAR Data Pre-processing

SAR data includes unwanted radiometric noise and geometric distortion. Preprocessing of SAR images needs to be performed for a wide range of applications. Speckle noise reduction and geometric correction need to be removed by several preprocessing steps. The geometry of the Earth's surface in an image looks different from point to point in the range direction. Slant range distortion, geometric distortion(layover and foreshortening), radiometric distortion and speckle are the major factors that affect radar backscatter [27].

The side-looking nature of radar results in geometric distortion or images. As the satellite moves from near range to far range, Earth's surface near the radar signal looks compressed and results in slant range distortion [27]. We need to calculate the proper ground range distance using the slant range distance and platform altitude. Slant range images need to be converted into ground range [27]. Due to relief displacement in Sentinel-1 radar images, they are subjected to geometric distortion: Layover and Foreshortening [27]. Due to the presence of mountains and hills on Earth's surface, radar signals from the top of the mountain return earlier compared to the bottom. As a result, the top of a mountain

image is displaced towards the radar. When the radar signals reach the base of a mountain before it reaches the top, foreshortening distortion occurs which results in an incorrect slope due to distortion. Both of these distortions result in shadows in radar images and can be corrected using Digital Elevation Model(DEM). The influence of topography on backscatter intensity needs to be corrected. Speckle is a noise that exists in SAR images and it degrades the quality. It happens due to constructive and destructive interference from multiple scattering. Some pixels appear bright and some are darker due to speckles in images. Speckles can be removed by multi-looking or spatial filtering.

The preprocessing workflow of Sentinel-1 SAR images consists of 7 steps: applying orbit file, thermal noise reduction, border noise removal, calibration, range doppler terrain correction and conversion to dB [12]. An orbit file is applied to provide an accurate position of objects in SAR images. Orbit state vectors for each SAR scene are updated in the product metadata [12]. Thermal noise affects Sentinel-1 SAR image intensity, particularly in cross-polarization channels (VH and HV) [12]. Lookup Tables(LUT) provided by Sentinel-1 level-1 data are used to derive calibrated noise [12]. Low-intensity noise and invalid data present on scene edges need to be removed [12]. After removing border noise, digital pixel values should be converted to radiometrically calibrated SAR backscatter values [12]. Speckles present in calibrated images are removed to increase the quality of SAR images [12]. Varying incidence angles result in image distortion [12]. Terrain correction is applied to remove distortions from SAR images. Geometric distortions mentioned earlier are corrected using the digital elevation model [12]. The final step is to convert the backscatter coefficient to dB using a logarithmic transformation [12].

3.3 Polarisation and Backscatter Coefficient

Sentinel-1 has been dual-channelled to transmit and receive signals. Polarisation is commonly used to denote by two letters in SAR images, the first indicates the transmitted polarisation and the latter is received polarisation [29]. The light pulse can be transmitted and received at either vertical(V) or horizontal(H) polarization. VV(Vertical transmission; Vertical reception) and VH(Vertical transmission; Horizontal reception) are the two basic polarization bands that give us information about the surface backscatter at any given location. Radar signals are transmitted and received at vertical(V) or horizontal(H) polarisation [29]. Co-polarisation(VV and HH), and cross-polarisation(HV and VH) represents the backscatter intensities at any location [29]. Backscattering of radar signals gives us additional information about crop type, growth of crops, soil and structure of the crop [29]. Scattering can be originated from soil, water, vegetation or interaction between the three

in rice fields. Dielectric properties of the medium play an important role in the portion of radar signals returned back to the sensor. As the dielectric constant value increases, the backscatter value increases. Increasing moisture content increases the backscatter intensity. Direct backscatter, forward scattering, diffuse scattering, double-bounce scattering and volume scattering are the major scattering mechanisms of radar signals [29]. Specular reflection occurs on smooth surfaces; most of the incident energy is reflected away and those areas appear dark in SAR images. Specular reflection occurs in rivers without waves. Rough surfaces scatter or diffuse radar signals in all directions. As a result, rough surfaces in radar images appear brighter. When the rough surface is wet, it scatters energy more brightly. Urban areas have higher backscatter due to specular double bounce scattering of the energy and appear bright. H-polarized signals' energy return is stronger in vegetation than in bare soils [10]. Cross-polarization(VH) and co-polarization(VV) values are more sensitive to vegetation changes [10].

The sentinel-1 C-band data contains VH polarisation which provides information about rice growth [8]. *Truong et. al.* used Sentinel-1 VV and VH polarisations for mapping vegetation type in Dalak, Vietnam by calculating σ°_{VV} + σ°_{VH}, σ°_{VV} - σ°_{VH}, σ°_{VV}/ σ°_{VH} and RVI4S1. SVM (Support Vector Machine) was used to categorise the fields. Polarisation intensity ratio $\sigma^{\circ}_{VH}/\sigma^{\circ}_{VV}$ is also considered to identify crop type and is sensitive to crop growth [16] [2]. VV polarisation is effective in analysing soil conditions while HH polarisation is best for water [11]. The correlation between rice growth parameters and the backscatter coefficient was analysed and found that VH polarization exhibits the best correlation [42]. While the correlation between VV backscattering coefficient and rice growth was found to be low [42]. The ratio of backscattering coefficients σ°_{VV} and σ°_{VH} was used for rice field mapping and a favourable result was obtained [42]. A high correlation value was obtained between backscattering coefficient σ°_{VH} and rice age [42]. While the correlation value between σ°_{VV} and rice age was found to be low [42].

3.4 Phenology

According to the International Rice Research Institute, the phenological phases of rice fields are categorised into three major phases: vegetative, reproductive, and ripening [21]. Three phases are then further classified into 9 different growth stages and are shown in Figure 3.1 [21]. The duration of these three phases depends on rice species, irrigation patterns and climate conditions. Figure 3.1 shows detailed information about rice phenological phases and the number of days for each phase. Information about rice phenological development plays an important role in plant growth and development. The average life

cycle of tropical rice is about 110-120 days [21]. The number of times rice is cultivated per year depends on the climate conditions and rice species. Rice can be cultivated three times a year under tropical conditions with optimal irrigation [21]. The approximate days for the vegetative, reproductive, and ripening phases are 65, 35 and 30 days respectively [21].

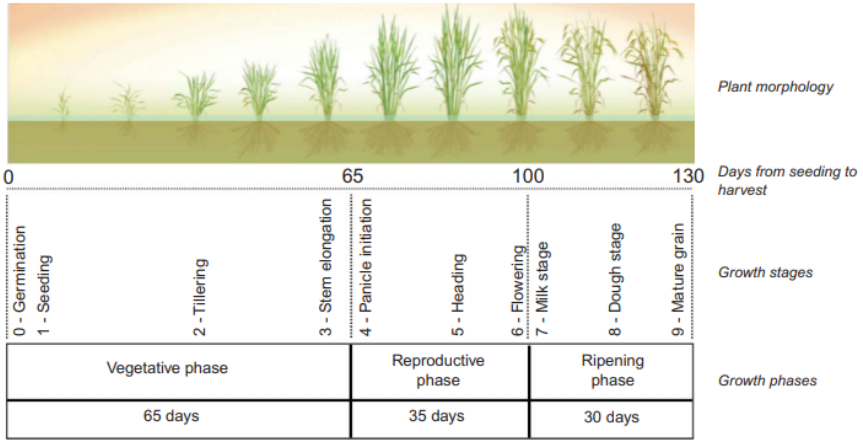

Figure 3.1: Rice Phenological stage Source: International Rice Research Institute

Canopy structure(stem, leaves and ears) and underlying soil surface of rice fields greatly influence scattering [21]. Additionally, plant height, biomass, and the presence of water also influence the scattering of radar signals [21]. The rice crop growth cycle can be tracked using sentinel-1 SAR images over the time period. Early stage, the seedling stage might see less scattering due to reflection from flooded fields and background soil [21]. Flooded fields provide low VV and VH backscatter intensities. During the first week of transplanting rice, the area covered by rice is less than 15% and reflectance is caused by soil and water [21]. The backscatter coefficient also increases with the growth of rice. The scattering intensity of radar signals peaks during the flowering stage due to dense vegetation, whereas the mature stage before harvesting sees a drop in scattering due to the formation of rice tassels [21]. Backscattering of radar signals varies from the pre-vegetative stage to the post-harvesting stage in rice fields [6]. With the significant difference in scattering between flooded and non-flooded fields, it is easy to distinguish rice fields [6]. As rice plant grows mature, the vegetation index increases significantly and reaches a maximum at the heading stage [6]. During the ripening stage, the presence of grains and a decrease in vegetation water content, results decrease in scattering and reaches its lowest [6]. Variations in backscatter intensity are higher in rice crop fields compared to any other fields [6]. VV-polarised backscatter coefficient value is higher compared to HH-polarised backscatter coefficient value during the initial stage due to short vertical leaves and stems [1]. VV-polarised backscatter coefficient value decreases as the rice crop ma-

tures and the value is less than the HH-polarised value [1]. Variation of the backscatter coefficient is the key to identifying the rice fields [21].

The rice crop calendar in An Giang province is not uniform and the number of crop cycles depends upon the type of rice planted [33]. Our study area is An Giang province, Vietnam, and has a complex cropping pattern [33]. *Hoa et. al.* used X-band SAR data to identify paddy fields, and sowing dates and categorise crop cycles(short and long) using radar backscatter and rice parameters [33]. The average farm size in the region is about 1 to 2 hectares and cultivates three major cropping seasons per year: winter-spring, summer-autumn and autumn-winter [33]. The three seasons can also be classified as early season, mid-season and longer rainy season and the transplanting dates for these crop seasons are November, April and July respectively [33].

3.5 Vegetation Indices

Different Vegetation Indices(VI) are derived from satellite images to examine the vegetation status. Normalized Difference Vegetation Index(NDVI), Enhanced Vegetation Index(EVI) and Soil Adjusted Vegetation Index(SAVI) are calculated from optical satellite images. While Radar Vegetation Index (RVI) is used for SAR radar images. The first attempt to calculate RVI using radar scattering from vegetation was done by Kim and Van Zyl [18]. Using vegetation indices, crop health, crop types and crop yield can be predicted. To estimate the vegetation water content of crops(rice and soybean), Radar Vegetation Index(RVI) was used [22]. RVI was proposed to identify the vegetation growth of rice and soybean fields and found that it has low sensitivity to environmental conditions [33]. The backscattering coefficient using C-, L- and X-bands were used to calculate vegetation indices(RVI) and Vegetation Water Content(VWC) was observed during crop growth cycles [33]. *Abdurrahman et. al.* calculated NDVI from optical images and RVI from SAR images and found a good correlation between these two vegetation indices. Radarsat-2 data were pre-processed and four bands(HH, HV, VH and VV) sigma scattering coefficients were used to calculate the RVI [36]. They further concluded that soil condition and structure can also be identified using vegetation indices [36]. NDVI values obtained are found to be highly correlated with VH polarisation and polarisation ratio(VH/VV) [4]. In order to calculate the vegetation index using sentinel-1 data, RVI(RVI4S1) is found to be effective [35]. RVI is measured between 0 and 1 and measures radar signal scattering [36]. RVI score for the bare smooth surface is close to 0 and the value increases as vegetation grows [36]. The value of RVI depends on the canopy structure, orientation and dielectric property of a field [36].

3.6 Related Research and Applied Machine Learning Algorithms

With the availability of remote-sensing images and machine-learning algorithms, monitoring and identifying agricultural fields become a trend. Multi-temporal Landsat 8 optical images were used to map paddy fields using deep learning Convolutional Neural Network(CNN) [25]. Normalized Difference Vegetation Index(NDVI) was calculated using Landsat images to identify double-cropping rice and single-cropping rice [37]. Most studies were carried out using optical satellite images to identify rice fields and received fairly good accuracies. Vegetation indices(NDVI, EVI, SAVI) were calculated from Sentinel-2 optical images and used to predict rice yields using linear regression and Artificial Neural Network(ANN) in Pakistan [3]. Another research was carried out to predict rice yield at pixel scale using a hybrid structure of long-short term memory(LSTM) and a One-dimensional Convolutional Neural Network(1D-CNN) in South Korea [19].

Sentinel-1 SAR time-series images were used to detect paddy fields in Thailand using the U-Net model [39]. The proposed model extracts the temporal statistical features of SAR images to identify paddy fields nationwide more accurately [39]. The variance of σ°_{VH} and σ°_{VV} scattering coefficient values for rice fields was found to be high compared to water bodies [39]. Backscattering coefficient values of fields were analysed using Decision Tree(DT) and Random Forest(RF) models to predict the rice fields [9]. Time-series σ°_{VV} and σ°_{VH} polarization values were used and observed and found that the rice fields have different temporal behaviour compared to other fields [9]. Rice fields were identified using 3 metrics: the variance of the VV/VH time series, the slope of the linear regression of the VH time series and the Gaussian profile of the VV/VH time series [9]. Another research carried out in Hanoi, Vietnam used RF algorithm and Sentinel-1 SAR time-series polarisation data using VV, VH and VV/VH to detect paddy fields [38]. Double and single rice crops were mapped and found that the VV/VH feature achieved the highest accuracy at about 95.5% [38]. Results obtained from time-series SAR data with a resolution of 20 metres for both VV and VH polarisations were found to be less effective compared to 10 metres [38]. The overall accuracy of 83% was obtained using DT when VH polarisation was used to detect rice fields. The main reason to choose HV over VV was due to the high dynamic range of backscattering [28].

A deep Neural Network(DNN) tries to mimic the human brain by combining inputs, weights and bias. DNN consists of a neural network of more than 3 layers: input, hidden and output. It extracts feature information and the relationship between features to predict the output. DNN are widely used in image [32], text [34] and audio [41] analysis. However, for tabular data tree-based algorithms are mainly used to predict the output. Tra-

ditional DNNs have too many parameters and lack proper inductive bias so they cannot be used for tabular data [5]. Tree-based algorithms are good at picking global features based on the statistical information gained [5]. XGBoost, and LightGBM are widely used ensemble Decision Tree(DT) approaches for tabular data to increase the accuracy of the model. Tree-based algorithms can be outperformed by using deep learning to enhance the representation capacity while retaining their feature-selecting property [5].

DNN algorithms enable gradient descent-based end-to-end learning for tabular data and help the efficient encoding of features, removing the need for feature engineering and representation learning [5]. There are a few benefits of the TabNet algorithm and it really works well in the case of tabular data. Firstly, it trains raw data using gradient descent-based optimization and removes the need for feature engineering [5]. Secondly, at each decision steps it selects features using sequential attention enabling interpretability(local and global) and better learning [5]. Local interpretability lets us visualize how important the features are and how they are combined [5]. While global interpretability measures the contribution of each feature [5]. Finally, it adds the benefit of unsupervised pre-training in order to predict the masked features [5].

3.7 Scaling Operations and Calculations

Earth observation(EO) data can be overwhelming for most software and requires huge computing power. Information about backscattering coefficient values at particular locations contains coordinates(latitude, longitude) and time values. Satellite images have huge dimensions. We need to arrange them in a way that data extraction will be easy and efficient. An EO data cube is being widely used and adopted for large collections of satellite images [7]. These data cubes can be modelled as multidimensional data to support time-series analysis [7]. EO data cubes are nothing but collections of images of a specific location over a particular time period [7]. Sentinel-1 polarisations VV and VH for a particular location at a given time period need to be extracted. To work with this multi-dimensional data, we need to use xarray [15]. Xarray is designed to work with labelled multidimensional data inspired by pandas and used for self-described scientific data. As the amount of data increases calculation takes time and we will run out of memory. To work with huge data in parallel, we need to divide our data into smaller chunks and Dask allows us to do that [33].

CHAPTER 4

Research Methodology

Difficulties in mapping paddy fields in Vietnam lie in two aspects. Firstly, clouds in Vietnam are persistent and cover rice fields most of the year. As a result, optical satellite images are affected by clouds and leading to low accuracy in prediction. Secondly, intense farming makes it difficult to identify the relationship between rice phenology and backscattering due to diverse cultivation patterns. As a solution, in this paper, the TabNet algorithm is used to identify the rice fields using Sentinel-1 RTC time-series data. The below flowchart diagram Figure 4.1 shows the proposed solution. First, Sentinel-1 RTC data from Microsoft Planetary Computer were accessed. Preprocessing of SAR images is already performed and data are ready to use. Several features derived from two polarisation values are then given input to a deep tabular learning algorithm, TabNet. TabNet model was adopted to train the paddy rice prediction model using features.

4.1 System Design

4.1.1 Data Source and Pre-processing

With the successful launches of Sentinel-1A and Sentinel-1B, it offers large-scale land cover monitoring every 12 days [12]. In this study, Sentinel-1 satellite data were used. Sentinel satellites are part of the European Space Agency(ESA) space program. Data from Sentinel satellites can be downloaded freely from Copernicus Open Access Hub [12]. The Sentinel-1 mission has two satellites operating day and night and uses the c-band synthetic aperture radar imaging technique to record an image of the earth's surface. In order to use radar images, radiometric distortion and the influence of topography on backscatter must be corrected [12].

Sentinel-1 RTC data are available in Microsoft Planetary Computer and are derived from Level-1 Ground Range Detected(GRD) products produced by European Space Agency

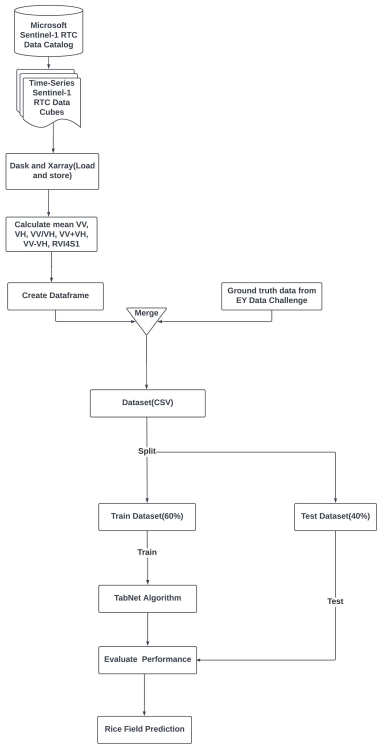

Figure 4.1: Proposed system design

(ESA) [26]. These data are preprocessed and stored as GeoTIFF(COG). Using a conversion algorithm, level-1 GRD products are converted into calibrated intensity [26]. Gamma correction values of flat earth are extracted from GRD metadata. Available polarizations are corrected in two dimensions using calibration coefficient and written in separate layers of a single file [26]. The resulting data is then radiometrically corrected using Planet-DEM as an elevation source. Out of four modes, RTC data is processed only for the Interferometric Wide Swath (IW) [26]. VV and VH polarisation values available in the Microsoft data catalogue are gamma-nought values and these values are obtained by normalizing sigma-nought with respect to the incidence angle. Obtained co-polarisation(γ°_{VV}) and cross-polarisation (γ°_{VH}) values were used in our experiment to detect the rice fields.

Quantitative analysis was performed to identify paddy fields using Sentinel-1 data. Obtained Sentinel-1 RTC data were provided by Microsoft Planetary Computer, which was derived from level-1 GRD data provided by ESA [26]. RTC data in the planetary computer were processed by Catalyst. RTC data Obtained for our research is only processed for the Interferometric Wide Swath (IW) mode, the main acquisition mode for land. Polarisations also known as data assets: γ°_{VV} and γ°_{VH} were used to identify the relationship between the backscattering coefficient and phenological phases of rice. The sentinel-1 RTC dataset is

available in Azure Blob Storage and was accessed by using pystac-client library.

4.1.2 Accessing Sentinel-1 Data

Data starting from December 2021 to November 2022 were obtained for 600 different locations. 1-year data were gathered to capture 3 rice crop cycles. First, the area of interest was defined for all locations using the latitude and longitude values. The area of interest will cover approximately a 5x5 pixel region and each pixel resolution is 10 meters, which is a baseline accuracy for our data. The backscatter intensity of 250 square meters was accessed and aggregated by the mean value. Library, pystac_client was used to search items on the Microsoft Planetary Computer STAC endpoint. All matched scenes based on our criteria(area of interest, time, assets) were listed. Data were clipped based on the area of interest and time frame. Clipped data assets(VV and VH) were loaded into Open Data Cube(ODC) using the API stac_load. Daskbacked arrays are internally connected instead of loading pixels directly. Xarray dataset was obtained which has 3 dimensions: latitude, longitude and time. Mean γ°_{VV}, γ°_{VH} and RVI4S1 values were calculated using dimensions(latitude and longitude). Xarray datasets were then converted into Pandas series to create DataFrame. The resulting dataframe is then written into Comma-separated Values(CSV) file. Coordinate Reference System(CRS) EPSG:4326 was used for projection which is a standard for latitude-longitude in degrees. Obtained data then merged with the data provided in the competition and then written to a final CSV file.

4.1.3 Creating Features

Below lists all the calculations made during our research:

- VV
  This value is the terrain-corrected mean naught value(γ°_{VV}) of radar signal transmitted vertically and received with vertical polarization.

- VH
  This value is the terrain-corrected mean naught value(γ°_{VH}) of radar signal transmitted vertically and received with horizontal polarization.

- Month
  This feature contains the information of the month at which the image of a location is recorded. This value is useful in time series analysis to see how the values change over time.

- RVI4S1
  The radar vegetation index(RVI4S1) has been used to monitor the level of vegetation growth using time-series satellite data. The lowest value of the vegetation index indicates the bare surface and the value increases as the crop grows [35]. At first, Degree of Polarisation(DOP) was calculated and then RVI4S1 value was calculated as shown below:
  DOP =
  $$\frac{\gamma^{\circ}_{VV}}{\gamma^{\circ}_{VV} + \gamma^{\circ}_{VH}}$$
  RVI4S1 =
  $$\sqrt{DOP} * \frac{4 * \gamma^{\circ}_{VH}}{\gamma^{\circ}_{VV} + \gamma^{\circ}_{VH}}$$

- VRAT calculates the ratio of VV and VH polarisations.

  VRAT =
  $$\frac{\gamma^{\circ}_{VV}}{\gamma^{\circ}_{VH}}$$

- SPAN
  Span calculates the total polarimetric power and can be obtained by adding VV and VH. SPAN = γ°_{VV} + γ°_{VH}

- Difference
  It represents the difference in polarimetric power and can be calculated by subtracting VH from VV. diff = γ°_{VV} - γ°_{VH}

4.1.4 Merging Datasets

Obtained CSV file containing features was merged with the ground truth data provided by EY Data Challenge 2023. The final dataset contains 36600 rows. Sentinel-1 data were available for 61 different days for 600 locations during our period.

4.1.5 Splitting Dataset

The dataset obtained was divided into two subsets: train and test to evaluate the performance of our model. Of the total data, 60% were used for training our model, while

40% were used to validate our model. Splitting the dataset adds benefits and lets us know how well our model predicts using unseen data.

4.1.6 TabNet Architecture

TabNet is a deep tabular data learning algorithm [5]. TabNet consists encoder and a decoder. TabNet encoder consists of a feature transformer and an attentive transformer. Feature transformer consists of 4 blocks of Fully Connected Layer(FC), Batch Normalization(BN) and Gated Linear Unit(GLU). FC layer is used for learning non-linear combinations of input features. BN makes neural networks faster by standardizing and normalizing the features. While GLU is an activation function and learns faster compared to the sigmoid. GLU allows hidden units to communicate deeper and prevents vanishing gradients in a model. Shared blocks in the feature transformer allow to reuse of the weights and reduce the parameters in the model for better generalisation. The attentive transformer uses sparse-matrix to select features. Feature selection mask provides information about the functionality of the model and can be aggregated to obtain global feature importance [5]. The attentive transformer block calculates how much each feature has been used in prior decision steps [5].

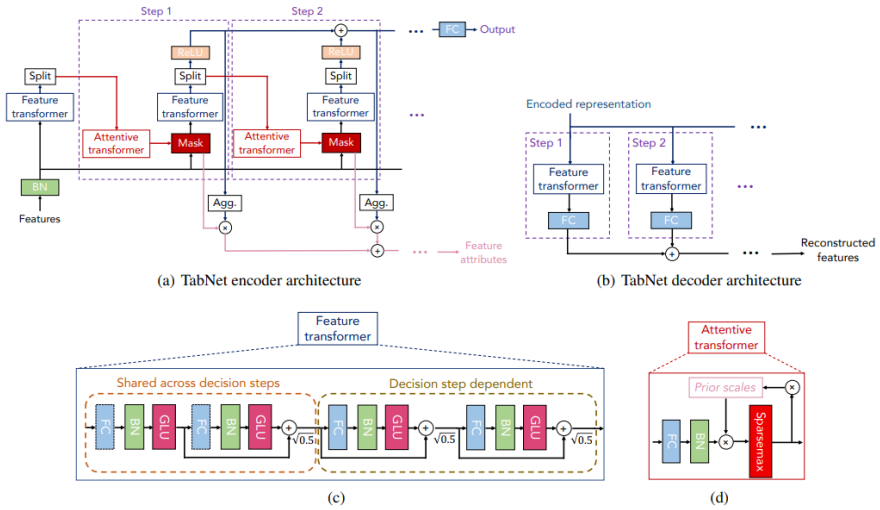

Figure 4.2: TabNet Architecture Source: [5]

4.1.7 Evaluation of Performance

In order to evaluate the performance of the model and to know how well it predicted the output, accuracy, precision, F1-score and recall values were calculated. A confusion

matrix was used to evaluate our binary classification model. To construct a confusion matrix, following values are calculated as shown below:

- True Positive: Number of positive outputs which are classified accurately.

- True Negative: Number of negative outputs classified accurately.

- False Positive: Number of actual negative outputs classified as positive.

- False Negative: Number of actual positive outputs classified as negative.

All 4 values calculated above are used to measure the value for accuracy, precision, recall and f1 score.

- Accuracy
  The accuracy score lets us know the total number of times our model predicted the correct result for all the output classes.
  Accuracy =
  $$\frac{TruePositive + TrueNegative}{TruePositive + TrueNegative + FalsePositive + FalseNegative}$$

- Precision
  To know how good our model is at predicting a specific output category.
  Precision =
  $$\frac{TruePositive}{TruePositive + FalsePositive}$$

- Recall
  Recall lets us know about the ability of a model to detect positive samples or output classes.
  Recall =
  $$\frac{TruePositive}{TruePositive + FalseNegative}$$

- F1 Score It combines precision and recall scores to calculate the accuracy of a model.
  F1 Score = $$\frac{2 * Precision * Recall}{Precision + Recall}$$

4.2 Handling Missing and Null Values

Some pixel values in Sentinel-1 RTC data were missing due to numerous factors such as shadow. Missing values for VV and VH polarisation in Sentinel-1 RTC data are represented by -32768. Missing values of a particular location in our data were replaced by the recent previous values.

4.3 Feature Scaling

Feature scaling is a preprocessing technique of scaling numerical features on a uniform scale. Feature scaling helps the machine learning model to perform better. The most common feature scaling techniques are standardization, min-max and normalization scaling. A standard scaler is used to standardize all features by removing the mean value and scaling data to unit variance.

4.4 Hyperparameters

Below table 4.1 lists all the hyper-parameters used for our TabNet model.

Hyperparameter	**Value**
Batch Size	512
Learning Rate	0.02
Optimizer Type	Adam
Epochs	100
Seeds	42
Scheduler step size	10
Scheduler gamma	0.9
Lambda Sparse	0.001
Mask Type	Sparsemax
Number of steps	3

Table 4.1: Hyperparameters values for TabNet model

4.5 Tools and Libraries Used

Throughout the research lot of tools and libraries to collect data, process data, visualize data, create a model and evaluate the result of our machine-learning model. Table 4.2 lists the major tools and libraries used in our research.

Tool/Libraries	**Used For**
Pytorch TabNet	Train the model
Dask	Accessing data parallelly
Xarray	Access labelled multi-dimensional array
Pandas	Used to explore, analyze, clean and manipulate data.
Matplotlib, Seaborn and Folium	Visualize data
PyStac	To access SpatioTemporal Asset Catalog(STAC)
Scikit-learn	Model evaluation and splitting data
Python	Programming language

Table 4.2: Tools and Libraries Used

CHAPTER 5

Analysis and Results

5.1 Analysis

Rice fields(ROI1 and ROI2) can be clearly distinguished from non-rice fields and 3 bell-shaped curves for each field can be observed from figures 5.1(a), 5.1(b) and 5.1(c). Those 3 bell-shaped curves show that those rice fields were cultivated 3 times that year. In Figures 5.1(a) and 5.1(b), the γ°_{VV} and γ°_{VH} backscattering coefficient of the river was found low and represented by the green line(ROI3). This is due to the specular reflection of radar signals on the surface of the river. The red line(ROI4) in Figure 5.1(a) and Figure 5.2(b) represents the γ°_{VV} and γ°_{VH} respectively. ROI4 represents a residential building covered by trees. Due to the volume and double bounce scattering of radar signals, VV and VH polarisation values are high for ROI4. VV and VH backscattering of buildings are high due to double bounce scattering. Another ROI(ROI5) represents a forest area and has dense vegetation. Volume scattering occurs on twigs and branches within a forest canopy. As a result, VV and VH values are higher compared to other locations.

The vegetation index(RVI4S1) value of rice fields(ROI1 and ROI2) are at their peak in the months of April, July and October. When the field is ploughed and rice is planted, the field has a low RVI4S1 value due to less vegetation. As vegetation grew and developed to the reproductive stage, the vegetation index value reached its maximum value. As rice plants reached the ripening stage, the water content in vegetation decreases. As a result, the RVI4S1 value reaches a low during the harvesting stage. The vegetation index value of ROI5 is higher compared to other fields due to the dense forest canopy. RVI4S1 value of ROI5 during the winter season is low. VV polarisation (γ°_{VV}) is affected by surface scattering and the double-bounce mechanism [40].

Here are some of the findings we observed from the research. Figures 5.1(a), 5.1(b) and 5.1(c) clearly show that rice fields(ROI1 and ROI2) were cultivated 3 times a year: the first was from November to April, the second was from April to August and the third one

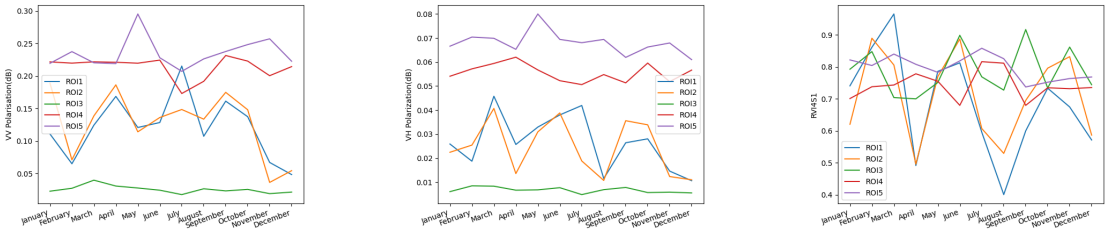

(a) VV Scattering (b) VH Scattering (c) Radar Vegetation Index

Figure 5.1: VV, VH and RVI Over Time

was from August to November. Harvesting and transplanting of rice was mainly done in April, August and December.

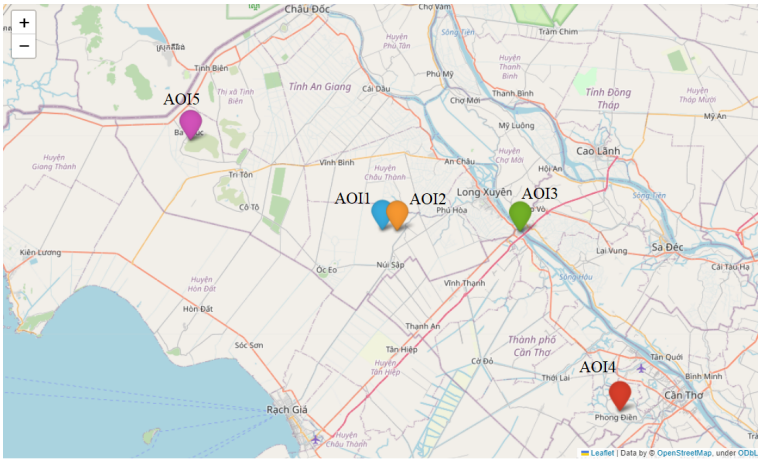

Figure 5.2: Our 5 Areas of Interest

5.2 Descriptive Statistics

The rice fields' Inter Quartile Range(IQR) values for VV, VH and RVI are 0.114, 0.024 and 0.47 respectively. While the non-rice fields' IQR values for VV, VH and RVI are 0.25, 0.058 and 0.2512 respectively. Dispersion of VH and VV polarisations of non-rice fields is higher compared to rice fields. Additionally, the dispersion of the RVI value of rice fields is high compared to non-rice fields. We also observed from Figure 5.3 that the IQR value of VH polarisation throughout the year is almost identical for non-rice fields while the values for rice fields vary every month.

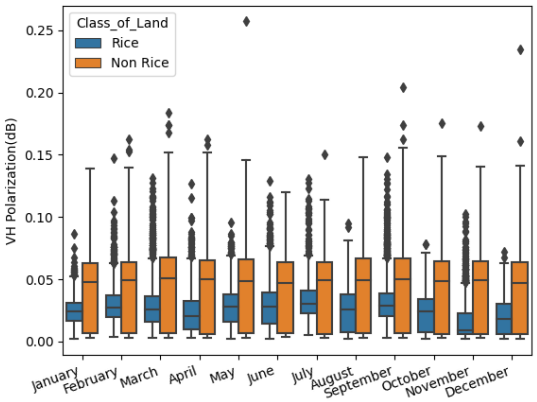

Figure 5.3: Mean VH Polarisation of rice and non-rice fields

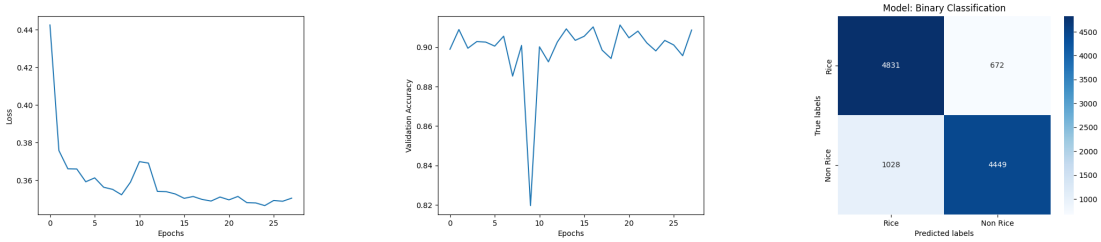

(a) Loss (b) Accuracy (c) Confusion Matrix

Figure 5.4: Performance of our model

5.3 Loss and Accuracy

TabNet classifier stopped early at epoch 27 after getting the best validation accuracy and loss value of 84.5% and 18% respectively. The accuracy score dropped dramatically at epoch 9 and increased significantly to reach the maximum at epoch 27 as can be seen in Figure 5.4(b). The loss of our model decreased steeply during the first five epochs and remained almost steady after epoch 15 as can be seen in Figure 5.4(a).

5.4 Results

Sentinel-1 time-series SAR data and a deep tabular learning algorithm, TabNet were used to solve the difficulties in identifying rice fields caused by complicated rice cycles in a tropical zone like An Giang. RVI4S1, VRAT, month and SPAN values are calculated by extracting γ°_{VV} and γ°_{VH} polarisations. The deep tabular learning algorithm, TabNet was proposed to learn the backscatter pattern of rice fields accurately. Our model TabNet classifier is a binary classification supervised algorithm. Radar Vegetation Index(RVI4S1)

values of rice fields were minimum at the transplanting phase and increased gradually with the increase in rice vegetation (Figure 5.1 c). The RVI4S1 value reached a peak and maintained a high value during the post-vegetative and reproductive periods. After the rice ripened, the RVI4S1 values started declining and reached their lowest during harvesting. Transplanting and harvesting dates were detected using polarization and RVI4S1 values. To verify the effectiveness of our model accuracy, precision, recall and F1 Score were calculated and the values obtained are 84.5%, 81.2%, 86.8% and 83.9% respectively. Exploratory data analysis was performed using a line graph and box plot to see how values change over time. IQR values of non-rice fields were found almost the same throughout the year while the values of rice fields vary. We also found that γ°_{VH} polarisation has the highest coefficient value compared to γ°_{VV}, and can be very useful for mapping rice fields. Additionally, the backscattering coefficient values of the river were found to be low among all.

CHAPTER 6

Discussion and Conclusion

Rice is one of the world's most important staples, and precise estimation of rice fields using satellite images is the key to the challenges in food security. This study proposes a system to identify paddy rice fields using Sentinel-1 backscattering response and RVI. This research mainly contributes to detecting rice fields using Sentinel-1 time-series SAR data. This study proposes a system to detect rice fields based on time-series Sentinel-1 data and a deep tabular learning algorithm in a tropical climate zone. TabNet model is proposed to accurately learn the backscattering pattern of rice fields in various stages. The result obtained from the classification algorithm based on Sentinel-1 data is impressive. These results showed that the proposed system can detect rice fields well in tropical areas. VH polarisation value is found to be highly correlated compared to VV polarisation. Various phenological phases of rice were determined using polarisation values using time-series data. This study also showed that harvesting and transplanting dates can be easily detected for individual fields based on the backscattering intensities and RVI. Additionally, it can help farmers analyze rice fields' vegetation index at critical time spans and allow them to take corrective and preventive actions.

However, Sentinel-2 optical images are not considered in this study. Further study will continue on how Sentinel-2 optical images will be used after filtering clouds. We still think that the accuracy can be increased by combining Sentinel-1 radar and Sentinel-2 optical data. Combining optical satellite data with radar data would be an interesting topic for further study.

Bibliography

[1] High angular resolution measurements of the monostatic backscattering coefficient of rice fields. 2009.

[2] Emilie Beriaux, Alban Jago, Cozmin Lucau-Danila, Viviane Planchon 1 and Pierre Defourny. Sentinel-1 time series for crop identification in the framework of the future cap monitoring. 2021.

[3] Saleem Ullah, Zulfiqar Ahmad Saqib, Azhar Abbas, Asad Ali, Muhammad Shahid Iqbal, Khalid Hussain, Muhammad Shakir, Munawar Shah Abid Nazir and Muhammad Usman Butt. Estimation and forecasting of rice yield using phenology-based algorithm and linear regression model on sentinel-ii satellite data. 2021.

[4] J. Alvarez-Mozos, J. Villanueva, M. Arias and M. Gonzalez-Audicana. Correlation between ndvi and sentinel-1 derived features for maize. 2021.

[5] Sercan O. Arık and Tomas Pfister. Tabnet: Attentive interpretable tabular learning. 2019.

[6] Chen C. and H. McNairn. A neural network integrated approach for rice crop monitoring. 2006.

[7] Rolf Simoes, Gilberto Camara, Gilberto Queiroz, Felipe Souza, Pedro R. Andrade, Lorena Santos, Alexandre Carvalho and Karine Ferreira. Satellite image time series analysis for big earth observation data.

[8] Mo Wang, Jing Wang, Li Chen, and Zhigang Du. Mapping paddy rice and rice phenology with sentinel-1 sar time series using a unified dynamic programming framework.

[9] Hassan Bazzi, Nicolas Baghdadi, Mohammad El Hajj, Mehrez Zribi, Dinh Ho Tong Minh, Emile Ndikumana, Dominique Courault and Hatem Belhouchette. Mapping paddy rice using sentinel-1 sar time series in camargue, france. 2019.

[10] Mariette Vreugdenhil, Claudio Navacchi, Bernhard Bauer-Marschallinger, Sebastian Hahn, Susan Steele-Dunne, Isabella Pfeil, Wouter Dorigo and Wolfgang Wagner. Sentinel-1 cross ratio and vegetation optical depth: A comparison over europe. 2020.

[11] Qi Gao, Mehrez Zribi, Maria Jose Escorihuela and Nicolas Baghdadi. Synergetic use of sentinel-1 and sentinel-2 data for soil moisture mapping at 100 m resolution. 2017.

[12] Federico Filipponi. Sentinel-1 grd preprocessing workflow. 2019.

[13] Olaf Ronneberger, Philipp Fischer, and Thomas Brox. U-net: Convolutional networks for biomedical image segmentation. 2015.

[14] Mohammad Saadat, Seyd Teymoor Seydi, Mahdi Hasanlou and Saeid Homayouni. A convolutional neural network method for rice mapping using time-series of sentinel-1 and sentinel-2 imagery. 2022.

[15] Stephan Hoyer1 and Joseph J. Hamman. xarray: N-d labelled arrays and datasets in python.

[16] Veloso A., Mermoz S., Bouvet A., Le Toan T., Planells M., Dejoux J. and E. Ceschia. Understanding the temporal behaviour of crops using sentinel-1 and sentinel-2-like data for agricultural applications. 2017.

[17] Alyssa K. Whitcraft, Inbal Becker-Reshefa, Christopher O. Justice, Lauren Gifford, Argyro Kavvada and Ian Jarvi. No pixel left behind: Toward integrating earth observations for agriculture into the united nations sustainable development goals framework.

[18] Y. Kim and J. J. van Zyl. A time-series approach to estimate soil moisture using polarimetric radar data. 2009.

[19] Seungtaek Jeong, Jonghan Ko and Jong-Min Yeom. Predicting rice yield at pixel scale through synthetic use of crop and deep learning models with satellite data in south and north korea. 2022.

[20] Duy Ba Nguyen, Kersten Clauss, Senmao Cao, Vahid Naeimi, Claudia Kuenzer and Wolfgang Wagner. Mapping rice seasonality in the mekong delta with multi-year envisat asar wsm data. 2015.

[21] Knauer K. Kuenzer C. Remote sensing of rice crop areas- a review. 2013.

[22] Yihyun Kim, Thomas Jackson, Rajat Bindlish, Hoonyol Lee and Sukyoung Hong. Radar vegetation index for estimating the vegetation water content of rice and soybean. 2012.

[23] Yaotong Cai, Hui Lin and Meng Zhang. Mapping paddy rice by the object-based random forest method using time series sentinel-1/sentinel-2 data. 2019.

[24] Dipankar Mandal. Radar vegetation index for sentinel-1 sar data - rvi4s1 script.

[25] Hui Lin, Guangxing Wang, Hua Sun Meng Zhang and Jing Fu. Mapping paddy rice using a convolutional neural network (cnn) with landsat 8 datasets in the dongting lake area, china. 2018.

[26] Microsoft. Sentinel 1 radiometrically terrain corrected (rtc).

[27] NASA. Applied remote sensing training program.

[28] K. Clauss, M. Ottinger and C. Kuenzer. Mapping rice areas with sentinel-1 time series and superpixel segmentation. 2017.

[29] Anjillyn Perez and Nestor Olfindo. A layman's interpretation guide to l-band (alos-2 palsar-2 global 25 m mosaics) and c-band (sentinel-1) synthetic aperture radar data.

[30] Christoph Szigarski, Thomas Jagdhuber, Martin Baur, Christian Thiel, Marie Parrens, Jean-Pierre Wigneron, Maria Piles and Dara Entekhabi. Analysis of the radar vegetation index and potential improvements. 2018.

[31] Ramón Torres, Ignacio Navas-Traver, David Bibby, Svein Lokas, Paul Snoeij, Björn Rommen, Steve Osborne, Francisco Ceba-Vega, Pierre Potin and Dirk Geudtner. Sentinel-1 sar system and mission.

[32] Kaiming He, Xiangyu Zhang, Shaoqing Ren and Jian Sun. Deep residual learning for image recognition. 2015.

[33] Matthew Rocklin. Dask: Parallel computation with blocked algorithms and task scheduling.

[34] Alexis Conneau, Holger Schwenk and Yann Le Cun. Very deep convolutional networks for text classification. 2017.

[35] Herman Snevajs, Karel Charvat, Vincent Onckelet, Jiri Kvapil, Frantisek Zadrazil, Hana Kubickova, Jana Seidlova and Iva Batrlova. Crop detection using time series of sentinel-2 and sentinel-1 and existing land parcel information systems. 2022.

[36] Abdurrahman G., Mehmet Sirac and Emrullah A. Comparison of ndvi and rvi vegetation indices using satellite images. 2019.

[37] Min Jiang, Liangjie Xin, Xiubin Li, Minghong Tan and Renjing Wang. Decreasing rice cropping intensity in southern china from 1990 to 2015. 2018.

[38] Kristofer Lasko, Krishna Prasad Vadrevu, Vinh Tuan Tran and Christopher Justice. Mapping double and single crop paddy rice with sentinel-1a at varying spatial scales and polarizations in hanoi, vietnam. 2018.

[39] Lu Xu, Hong Zhang, Chao Wang, Sisi Wei, Bo Zhang, Fan Wu and Yixian Tang. Paddy rice mapping in thailand using time-series sentinel-1 data and deep learning model. *MDPI Open Access Journal*, 2021.

[40] Lu Xu, Hong Zhang, Chao Wang, Sisi Wei, Bo Zhang, Fan Wu and Yixian Tang. Paddy rice mapping in thailand using time-series sentinel-1 data and deep learning model. 2021.

[41] Dario Amodei, Rishita Anubhai, Eric Battenberg, Carl Case, Jared Casper, Bryan Catanzaro, Jingdong Chen, Mike Chrzanowski, Adam Coates, Greg Diamos, Erich Elsen, Jesse Engel, Linxi Fan, Christopher Fougner, Tony Han, Awni Hannun, Billy Jun, Patrick LeGresley, Libby Lin, Sharan Narang, Andrew Ng, Sherjil Ozair, Ryan Prenger, Jonathan Raiman, Sanjeev Satheesh, David Seetapun, Shubho Sengupta, Yi Wang, Zhiqian Wang, Chong Wang, Bo Xiao, Dani Yogatama, Jun Zhan and Zhenyao Zhu. Deep speech 2: End-to-end speech recognition in english and mandarin. 2015.

[42] Fan Wu, Chao Wang, Hong Zhang, Bo Zhang and Yixian Tang. Rice crop monitoring in south china with radarsat-2 quad-polarization sar data. 2010.